Mutual Information for Registration of Monomodal Brain Images using Modified Adaptive Polar Transform

[1]D.Sasikala and [2]R.Neelaveni,
[1]Assistant Professor, Department of Computer Science & Engineering,
Bannari Amman Institute of Technology, Sathyamangalam, Tamilnadu, India -638401.
anjansasikala@gmail.com
[2]Assistant Professor, Department of Electrical & Electronics Engineering,
PSG College of Technology, Peelamedu, Coimbatore, Tamilnadu, India -641014.

Abstract: **Image registration has great significance in medicine, with a lot of techniques anticipated in it. This research work implies an approach for medical image registration that registers images of the mono modalities for CT or MRI images using Modified Adaptive Polar Transform (MAPT). The performance of the Adaptive Polar Transform (APT) with the proposed technique is examined. The results prove that MAPT performs better than APT technique. The proposed scheme not only reduces the source of errors and also reduces the elapsed time for registration of brain images. An analysis is presented for the medical image processing on mutual- information-based registration.**

Index Terms: **Adaptive Polar Transform; Gabor wavelet transform; Modified Adaptive Polar Transform; Modified Gabor wavelet transform; Registration; Brain Images.**

I.INTRODUCTION

Image registration is the method of superimposing images of the similar view captured at various times, from different perspectives, and/or by different sensors. The registration geometrically aligns two images (the model and sensed images). These approaches are classified based on their nature (area based and feature-based) and have four fundamental steps: (i) feature detection, (ii) feature matching, (iii) mapping function design, and (iv) image transformation and sampling. It is essential in all image analysis tasks in which the ultimate information is realized from the grouping of a range of data sources like in image fusion, change detection, and multichannel image restoration. Normally, required in medicine (combining CT and / or MRI data to obtain additional complete information about the patient, monitoring tumour growth, treatment verification, evaluation of the patient's data with anatomical atlases), and in computer vision (target localization, automatic quality control).

Many techniques of the image registration have been proposed previously. Medha V. Wyawahare *et al.* [1] proposed Image registration as a vital problem in medical imaging with applications in clinical diagnosis (Diagnosis of cardiac, retinal, pelvic, renal, abdomen, liver, tissue etc disorders). Ashok Veeraraghavan *et al.* [2] presented an approach for comparing two chains of deforming shapes by both parametric models like the autoregressive model and autoregressive moving average model and nonparametric methods based on Dynamic Time-Warping. Kendall's definition of shape is used for feature extraction. E.D. Castro and C. Morandi [3] placed steps for the new technique, based on the Fourier-Mellin transform. L. G. Brown [4] stated it as an intermediate step. J. P. Lewis [5] described it as cross correlation efficiently executed in the transform domain. S. Zokai and G.Wolberg [6] gave an idea about registration of multi resolution and multisensory images as a challenging problem in the research area of remote sensing and proposed new method for automatic affine image registration based on local descriptors, called automatic image registration by local descriptors (AIRLD). D. Lowe [11] presented a technique for extracting distinctive invariant features from images and achieves reliable matching among different views of an object or scene. J. B. Antoine Maintz et al. [12] presented a review of recent publications concerning medical image registration techniques. In probability and information theory, Mutual Information a dimensionless quantity with units of bits (sometimes known as transinformation) between two discrete random variables is termed as the amount of information shared between the two random variables. It can reduce the uncertainty. High Mutual Information (MI) indicates a large reduction in uncertainty; low MI indicates a small reduction; and zero MI between two random variables means they are independent.

$$I(X;Y) = \sum_{y\in Y}\sum_{x\in X} p(x,y)\log\left(\frac{p(x,y)}{p_1(x)\,p_2(y)}\right), \quad (1)$$

X and Y - Two discrete random variables.
$p(x,y)$ - Joint probability distribution function of X and Y.
$p1(x)$ and $p2(y)$ - Marginal probability distribution functions of X and Y respectively.

II. IMAGE REGISTRATION USING APT

A. *Localization*

The translation parameter between the two images was found. Fourier phase correlation is used to fix the translation before calculating the log-polar matching in the frequency domain. A study in [14] showed the aliasing problem by using

DOI: 01.IJNS.02.02.152

the phase magnitude of Fast Fourier Transform (FFT) to pick up the translation (of the centre point).

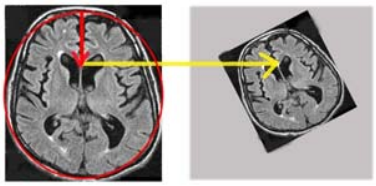

Fig 1. Feature point extraction and localization procedure for Transaxial T1 MR JPEG image of size 718 kB with resolution 1044 x 2219 pixels.

First, feature points are extracted from both the model and target image of a single modality, either CT or MRI. $P^M = \{p_1^M, \ldots, p_{nM}^M\}$ and $P^T = \{p_1^T, \ldots, p_{nT}^T\}$ are sets of feature points in the model and target image, respectively. The superscription and M and T denote the model and target image, and n_M and n_T are the number of feature points in the model and target image, respectively. To crop the model image out of the image, automatically one of the feature points is selected in the model image p_k^Me as a centre point for APT and chooses the size of the radius for the transformation R_{max} that adequately covers the model image to compute APT R^M and $È^M$ the projections of APT, R^M and $È^M$. On the left is the model image (*Brain Image* with the size 1044 x 2219 pixels) with 166 feature points identified. The model image is created by selecting one of the feature points in the model image p_k^Mas the origin, and is cropped to a circular image patch that covers the area R_{max} desired to be registered to the target image. On the right is the target image (*Brain Image* that is scaled by 0.7 and rotated by 30 degrees, the size of the image is 730x1553 pixels) with 180 feature points identified. To obtain the translation between the model and target image, the corresponding feature point $p_{k'}^M$ is located in the target image. As shown in Fig 1, the search space is limited to only a set of feature points in the target image, which is approximately 0.2% of the total number of pixels in the target image in this example. Hence, the search space is much smaller than that of the exhaustive search strategy.

B. *APT Matching*

After extracting feature points in the model image and selecting one feature point p_k^M as the centre point for computing the projections R^M and $È^M$ using the APT approach, the next step is to find the related feature point $p_{k'}^T$ in the target image and obtain both the scale and rotation parameters between the two images of the same modalities. Given a set of feature points in the target image and the radius size of the APT transform R_{max} to be identical as for computing the projections R^M and $È^M$, each feature point is applied in the target image as a centre point for computing APT creating the set of candidate projections $R^T = \{R_1^T, \ldots, R_{nT}^T\}$and $\theta^T = \{\theta_1^T, \ldots, \theta_{nT}^T\}$. By matching and with each member in the sets of projections R^M and $È^M$, respectively, the translation, scale, and rotation parameters are obtained concurrently. The matching results have three dimensions: the scale, rotation, and distance coefficient. The translation parameter is the offset involving the locations of to the feature point in the target image that defers the lowest distance coefficient.

For a given feature point p_z^T in the target image, I^M, I_z^T , R_z^T and θ_z^T are denoted as the model image, the image area that is cropped from the target image to be matched with the model image, projection on the radius coordinate, and angular coordinate, respectively. Then the scale change in the Cartesian coordinates reflects as variable-scalene of the projection, and rotation change reflects as shifting in the projection. Therefore, the new matching mechanisms are put forth to obtain both the scale and rotation parameters. The mathematical expression of image I_z^Tie, scaled and rotated version of image I^M is

$$I_z^T(x,y) = I^M(a_z x\cos\theta_z + a y\sin\theta_z, -a_z x\sin\theta_z + a_z y\cos\theta_z) \quad (2)$$

In the polar domain, (2) can be expressed as

$$I_z^T(r,\theta) = I^M(a_z r, \theta - \theta_z) \quad (3)$$

Where a_z and θ_z are the scale and rotation parameters, respectively. As shown in (2) and (3), the scale parameter a_z, in the Cartesian coordinates appears as scaling with the same value in the radius direction of the polar transformed image. For the case of adaptive sampling in APT, the outcome of scaling is seen in the Cartesian to APT mapping remains similar to that of the polar transform mapping. Except for APT, the number of samples in the angular direction can vary (adaptive).To calculate the 1D projection in the radius direction R(i), multiplication variable $Ù_i$ is initiated to compensate the effect of adaptive sampling in the angular direction. As a result, the 1D projection R of APT is an approximation to that of the polar transformed image.

$$R_z^T(i) = \Omega_i \sum_{j=1}^{n_{\theta i}} IP_z^T(i,j) \quad (4)$$

and $$R^M(i) = \Omega_i \sum_{j=1}^{n_{\theta i}} IP^M(i,j) \quad (5)$$

is obtained. R_z^T is calculated in terms of R^M as follows:

$$R_z^T(i) = \Omega_{a_z i} \sum_{j=1}^{n_{a_z i}} IP^M(a_z i, j) \quad (6)$$

$$R_z^T(i) = R^M(a_z i) \quad (7)$$

Thus, variable-scale a_z is a global and uniform scale for the 1D projection R curve. As shown in Fig. 2(a) and (c), the projections È of the scaled images in the Cartesian is a little altered compared with that of the original image because the areas enclosed during the APT transforms are unlike result of scaling. Hence, to obtain the shifting parameter involving the two projections $È^M$ and $È^T$and, variable-scale parameter a_z involving the two projections $R^M$and R_z^T must be obtained first.

B.A. Find Scale Parameter:

*D*epending on prerequisites of the application in terms of the computational cost, accuracy, image types and environments, two effective algorithms are initiated.

*Algorithm 1: Fourier Method: T*he Fourier transform of the scaled signal x (t) can be expressed as

$$x(t) \leftrightarrow x(\omega) \quad (8)$$

$$x(at) \leftrightarrow \frac{1}{|a|} X\left(\frac{\omega}{a}\right) \quad (9)$$

DOI: 01.IJNS.02.02.152

Similar to polar transform, the projection calculated from image I_z^T that is the scaled version of image I^M with the scale parameter a_z will also be scaled version of the projection with the same scale parameter a_z. From (8) and (9), given Fourier transform of the projection R(.) as Ã(.), the scale parameter $|a_z|$ obtained by

$$|a_z| = \frac{\Gamma^M(0)}{\Gamma_z^T(0)} \quad (11)$$

$$(a_z i) \quad (10)$$

This Fourier technique executes well only when the scale parameter is small. Large scale parameter defers the aliasing problem. Hence, this algorithm is apt for applications that involve fast and accurate image registration while the scale parameter involving the two images is expected to be small, such as medical image registration, or scene change detection.

Algorithm 2: Logarithm Method: The second algorithm applies the scale invariant property of the logarithm function. First, the logarithm function is applied to the projection R and the output is then quantized to maintain the original dimension of the projection. The mathematical expression of the operation is as follows:

$$\mathcal{L}R(k) = R\left(n_r \frac{\log k}{\log n_r}\right); k = 1, \ldots\ldots, n_r \quad (12)$$

The parameter LR (11) shows the logarithmic of the projection. Given image I_z^T a scaled and rotated version of image I^M, the scale parameter a_z involving the two images would shows translation in the logarithm domain

$$\pounds\mathcal{L}R_z^T(\rho) = \mathcal{L}R^M(\rho) + \log a_z \quad (13)$$

To find the displacement d, where d=log a_z, such that $\mathcal{L}R_z^T(\rho) = \mathcal{L}R^M(\rho - d)$, the correlation function can be assessed between the two logarithmic of projections $C(\mathcal{L}R^M, \mathcal{L}R_z^T)$

$$d = argmax\, C(\mathcal{L}R^M, \mathcal{L}R_z^T) \quad (14)$$

This algorithm defers high accuracy and fast matching in the general condition.

B.B. Find Rotation Parameter:

*N*ext step is to find the rotation parameter $\grave{e}_z$. For the same sampling radius, R_{max}, the larger the image (a_z>>1), the smaller the area of the scene is covered in the sampling procedure. As a result, the magnitude of the projections È between the two images could be slightly altered and detail is shown in Fig. 2(a) and (c). As a result, to precisely acquire the rotation parameter $\grave{e}_z$, (9) must be adapted according to the scale parameter a_z: examine (14) and (15). Both projections are then resampled to be equal in length. The rotation parameter can be found by evaluating the correlation function $C(\hat{\Theta}^M, \hat{\Theta}_z^T)$

$$\hat{d} = argmax\, C(\hat{\Theta}^M, \hat{\Theta}_z^T) \quad (15)$$

$$\theta_z = \frac{2\Pi\hat{d}}{\hat{n_\theta}} \quad (16)$$

B.C. Find Distance Coefficient:

The final important component resulting from APT matching is distance coefficient, denoted as $å_z$, which shows how large the variation is that involves two images. The distance coefficient $å_z$ between the model image I^M and the target image can be worked out from the Euclidean distance between the projections $\hat{\Theta}^M$ and $\hat{\Theta}_z^T$

$$\varepsilon_z = \sqrt{\sum_{i=1}^{\hat{n}_\theta}[\hat{\Theta}_z^T(i) - \hat{\Theta}^M(i - \hat{d})]^2} \quad (17)$$

For registration, a feature point is searched in the target image that corresponds with the feature point in the model image. Such feature point is the point that yields the lowest distance coefficient. The projections R^M and R_z^T are not used for computing the distance coefficient $å_z$ as the dimension of projections that can be utilized in the computation varies depending on the scaling parameter a_z. So, only projections $\hat{\Theta}^M$ and $\hat{\Theta}^T$ are used in the computation.

C. Image Comparison

Using advantages of APT, quick and simple comparison method is put forth that can effectively and automatically position the altered area or area where the registered image pair differs without further computational cost. Since the scale difference in the Cartesian coordinates between the model image and target image yields different area coverage in the transformation process, the dimension of the projection R for comparing the two images needs to be altered accordingly. Given the scale and rotation parameters between the model and target image as a_k^r and $\grave{e}_k^{'}$, respectively, the altered area is found as a set of pixels (X,Y) in the Cartesian coordinates, where X=x1,….,x_t, Y=y1,…,y_t, and parameter is number of pixels in the altered area as follows:

$$\varepsilon_{\Re}(i) = \left|\left|\Re_{k'}^T(i) - \Re_{res}^M(i)\right|\right| \begin{cases} for\ i = 1\ to\ n_r\ if\ a_{k'} \geq 1 \\ for\ i = 1\ to\ a_{k'}\eta_r\ if\ a_{k'} \leq 1 \end{cases} \quad (18)$$

$$\varepsilon_\Theta(j) = \left|\left|\hat{\Theta}_{k'}^T(j) - \hat{\Theta}^M(j - \hat{d})\right|\right|, for\ j = 1\ to\ \hat{n}_\theta \quad (19)$$

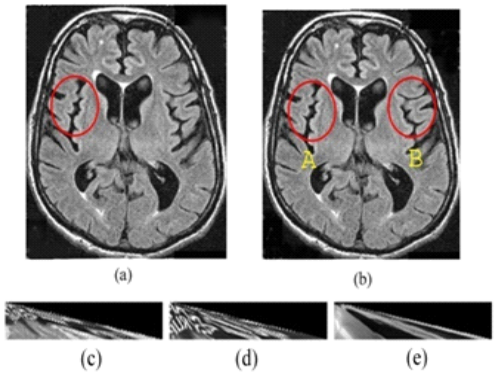

Fig 2. Example of the proposed image registration approach (a) model image where the model image is the area inside the circular line, (b) two candidates are chosen as examples using two feature points A and B of the target image, (c) APT of the model image, (d) and (e) APTs of the target image where the centre points of the transformation are feature points A and B, respectively.

The location of $p_{k'}^T$ is denoted in the Cartesian coordinates as (c_x ,c_y). For $\forall\varepsilon_R(i), \forall\varepsilon_\Theta(j) \geq \varepsilon$, set of image pixels is computed in the altered area (X,Y) as follows:

$$(X, Y) = \{(x_1, y_1), \ldots., (x_t, y_t)\} \quad (20)$$

$$\forall_{\varepsilon_\Re}(i), \forall_{\varepsilon_\Theta}(j) \geq \epsilon; \begin{cases} X = c_x + \varepsilon_\Re(i)\, sin\varepsilon_\Theta(j) \\ Y = c_y + \varepsilon_\Re(i)\, cos\varepsilon_\Theta(j) \end{cases} \quad (21)$$

DOI: 01.IJNS.02.02.152

The altered area can be recognized without extra computational cost.

$$\Theta^M = \begin{cases} \Theta^M, if\ a_z \le 1 \\ \sum_{i=1}^{n_r/a_z}[\eta_{ij}^1 IP^M\left(i, ceil\left(\frac{j-1}{\Omega_i}\right)\right) + \eta_{ij}^2 IP^M\left(i, ceil\left(\frac{j}{\Omega_i}\right)\right)], otherwise \end{cases} \quad (22)$$

$$\Theta_z^T = \begin{cases} \Theta_z^T, if\ a_z \ge 1 \\ \sum_{i=1}^{a_z n_r}[\eta_{ij}^1 IP_z^T\left(i, ceil\left(\frac{j-1}{\Omega_i}\right)\right) + \eta_{ij}^2 IP_z^T\left(i, ceil\left(\frac{j}{\Omega_i}\right)\right)], otherwise \end{cases} \quad (23)$$

Most registration algorithms, involving the 2D geometric transforms, additional computations are essential as post processes such as image alignment; transform both.Images to the same coordinates prior to the comparison, and image normalization. For the proposed approach, as both the model and target image are already transformed to the projections of APT domain, image comparison can be performed directly and simultaneously while obtaining scale and rotation parameters.

III.IMAGE REGISTRATION USING MAPT

A multiscale transform of a signal U may be defined as

$$U(b,a) = \int u(x)\,\varphi(x,b,a)\,dx, \quad (24)$$

Where a > 0 is the scale parameter, b is the time (or position) parameter.

TABLE I.
RESULTS FOR APT AND MAPT FOR BRAIN IMAGE

S. No	X in mm	Y in mm	Angle in degrees	Scaling In times	MI after registration for APT	MI after registration for MAPT
1	4	-10	9	0	0.6283	0.4895
2	-12	-7	13	0	0.6645	0.5446
3	5	-7	5	0	0.6416	0.5277
4	-14	-15	2	0	0.6796	0.5051
5	-8	-7	1	0	0.5287	0.5383
6	9	7	-7	0	0.6181	0.4636
7	7	-13	11	0	0.6483	0.4733
8	18	1	19	0	0.7023	0.5110
9	-17	0	-17	0	3.1481	3.1321
10	0	-9	12	0	0.6478	0.5144
11	23	-6	2	0	0.7553	0.5030
12	-15	5	-10	0	0.6352	0.5165
13	22	20	2	0	0.7897	0.4161
14	5	15	12	0	0.6414	0.4536
15	-21	16	-5	0	0.6792	0.4830
16	-1	19	13	0	1.2537	0.9999
17	5	10	-25	0	0.5586	0.3803
18	-3	11	25	0	0.9024	0.6436
19	11	-9	0	0	0.4833	0.4889
20	0	0	12	0	3.4928	3.4858
21	0	0	0	0	7.2870	7.3359
22	0	0	0	-4	7.2618	7.2982
23	0	0	0	-2	7.2670	7.3080
24	0	0	0	-3	7.2718	7.3149
25	0	0	0	1. 5	7.2784	7.3247
26	0	0	0	1. 25	7.2754	7.3206
27	0	0	90	0	3.1443	0.5279
28	0	0	180	0	7.2695	7.3128
29	0	0	270	0	0.5911	0.5263
30	0	0	270	-2	1.0038	1.0226
31	0	0	180	-2	2.2466	2.2699
32	0	0	90	-2	1.0168	1.0318
33	0	0	270	1. 25	2.0488	2.0777
34	0	0	180	1. 25	0.4824	0.4144
35	0	0	270	1. 25	1.7303	1.7596
36	4	-10	90	-2	0.9141	0.9219
37	-14	-15	180	-2	0.9224	0.9282
38	-15	5	270	-2	1.0991	1.0125
39	4	-10	90	1. 25	0.5114	0.4174
40	-14	-15	180	1. 25	0.5002	0.3774
41	-15	5	270	1. 25	0.5146	0.4452

In particular, analyzing function of Short-Time Fourier Transforms (STFT) using a Gaussian window (also known as Gabor transform).

$$\varphi_{STFT}(x,b,a) = e^{\frac{(x-b)^2}{2}} e^{ja(x-b)}, \quad (25)$$

where $j = \sqrt{-1}$. The analyzing function in wavelet transform using a Gabor wavelet (also called a Morletwavelet) is considered.

$$\varphi_{GWT}(x,b,a) = e^{\frac{(\frac{x-b}{a})^2}{2}} e^{j\omega_0(\frac{x-b}{a})}, \quad (26)$$

Where ù$_0$ is the basic frequency of ø$_{GWT}$. The Gabor and Gabor-wavelet transforms (GWT) are implemented to do local frequency analysis as they are well localized in the time and frequency domains. The Gabor and GWT analyze signals at different frequencies and scales in a dependent way, i.e., the frequency content range depends on working scale. This is undesirable for image analysis as the coding regions are characterized by a fixed periodicity that may occur at different scales. Neither of these transforms is suitable for such task.

$$\varphi_{MGWT}(x,b,a) = e^{-\frac{(x-b)^2}{2a^2}} e^{j\omega_0(x-b)} \quad (27)$$

Therefore, Modified Gabor Wavelet Transform (MGWT) is defined as a function of b and a as

$$U(b,a) = \int u(x)\, e^{-\frac{(x-b)^2}{2a^2}} e^{j\omega_0(x-b)}\, dx \quad (28)$$

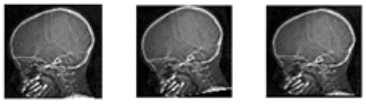

Fig 3. APT for CT Sagittal -432 x 427 – 41k JPEG, 36.3kB

Fig 4. MAPT for CT Sagittal-432 x 427 – 41k JPEG, 36.3kB

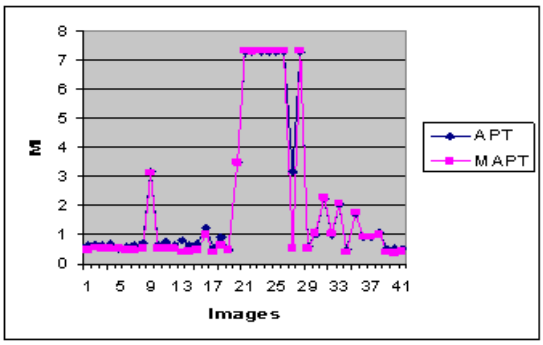

Fig 5. Comparison of APT and MAPT using MI.

DOI: 01.IJNS.02.02.152

IV. CONCLUSION

A series of experiments was performed using medical images different sizes. Registration of monomodal brain images using MRI- T1, T2 and CT scan images are studied and examined with regard to accuracy, robustness. For the algorithm evaluation, 41 such sets of CT image pairs were used. The results using MGWT in MAPT showed that scaled and rotated images registered well than the translated images. Further step is to implement a method that improves mutual information for translated images also.

REFERENCES

[1] Medha V. Wyawahare, Dr. Pradeep M. Patil, and Hemant K. Abhyankar, "Image Registration Techniques: An overview", International Journal of Signal Processing, Image Processing and Pattern Recognition Vol. 2, No.3, pp.1-5, September 2009.

[2] Ashok Veeraraghavan, "Matching Shape Sequences in Video with Applications in Human Movement Analysis" , IEEE Transactions on Pattern Analysis and Machine Intelligence, vol. 27 no. 12, pp. 1896-1909, December 2005

[3] E.D. Castro, C. Morandi, "Registration of translated and rotated images using finite Fourier transform", IEEE Transactions on Pattern Analysis and Machine Intelligence, vol.9, pp. 700–703, (1987).

[4] L. G. Brown, "A survey of image registration techniques," *ACM Comput. Surv.*, vol. 24, no. 4, pp. 325–376, Dec. 1992.

[5] J. P. Lewis, "Fast normalized cross-correlation," in *Proc. Vision Interface*, May 1995, pp. 120–123.

[6] S. Zokai and G.Wolberg, "Image registration using log-polar mappings for recovery of large-scale similarity and projective transformations," *IEEE Transaction in Image Processing*, vol. 14, no. 10, pp. 1422–1434, Oct. 2005.

[7] V. J. Traver and F. Pla, "Dealing with 2D translation estimation in log polar imagery," *Image Visual Computation*, vol. 21, no. 2, pp. 145–160, Feb. 2003.

[8] H. Araujo and J. M. Dias, "An introduction to the log-polar mapping," in *Proc. 2nd Workshop Cybernetic Vision*, Dec. 1996, pp. 139–144.

[9] H. S. Stone, B. Tao, and M. McGuire, "Analysis of image registration noise due to rotationally dependent aliasing," *J. Vis. Communication and Image Representation* vol. 14, no. 2, pp. 114–135, Jun. 2003.

[10] J. B. A. Maintz and M. A. Viergever, "A survey of medical image registration," *Medical Image Analysis*, vol. 2, no. 1, pp. 1–36, Mar. 1998.

[11] D. Lowe, "Distinctive image features from scale-invariant keypoints," *Int. J. Comput. Vis.*, vol. 60, no. 2, pp. 91–110, Nov. 2004.

[12] J. B. Antoine Maintz_ and Max A. Viergever," A Survey of Medical Image Registration," October 16, 1997

[13] J. Chen, H. Li, K. Sun, and B. Kim, "How Will Bioinformatics Impact Signal Processing Research," IEEE Signal Processing Magazine, vol. 20, no. 6, pp. 16-26, 2003.

[14] I. Grosse, H. Herzel, S.V. Buldyrev, and H.E. Stanley, "Species Independence of Mutual Information in Coding and Noncoding DNA," Physical Rev. E, vol. 61, no. 5, pp. 5624-5629, 2000.

[15] B.D. Silverman and R. Linsker, "A Measure of DNA Periodicity," J. Theoretical Biology, vol. 118, no. 3, pp. 295-300, 1986.

[16] W. Li, T.G. Marr, and K. Kaneko, "Understanding Long-Range Correlations in DNA Sequences," Physica D, vol. 75, pp. 392-416,1994.

[17] S. Datta and A. Asif, "A Fast DFT-Based Gene Prediction Algorithm for Identification of Protein Coding Regions," Proc. 30th IEEE Int'l Conf. Acoustics, Speech, and Signal Processing, vol. 3, pp. 113-116, 2005.

D.Sasikala is presently working as Assistant Professor, Department of CSE, Bannari Amman Institute of Technology, Sathyamangalam. She received B.E.(CSE) from Coimbatore Institute of Technology, Coimbatore and M.E. (CSE) from Manonmaniam Sundaranar University, Tirunelveli. She is now pursuing Phd in Image Processing. She has 11.5 years of teaching experience and has guided several UG and PG projects. She is a life member of ISTE. Her areas of interests are Image Processing, System Software, Artificial Intelligence, Compiler Design.

R. Neelaveni is presently working as a Assistant Professor, Department of EEE, PSG College of Technology, Coimbatore. She has a Bachelor's degree in ECE, a Master's degree in Applied Electronics and PhD in Biomedical Instrumentation. She has 19 years of teaching experience and has guided many UG and PG projects. Her research and teaching interests includes Applied Electronics, Analog VLSI, Computer Networks, and Biomedical Engineering. She is a Life member of Indian Society for Technical Education (ISTE). She has published several research papers in national and international Journals and Conferences.

DOI: 01.IJNS.02.02.152